Pergamon

Cement and Concrete Research 33 (2003) 747–753

CEMENT AND CONCRETE RESEARCH

On a qualitative relationship between degree of inhomogeneity and cold crushing strength of refractory castables

Jana Hubálková[a], Dietrich Stoyan[b,*]

[a]Department of Ceramic, Glass and Construction Materials, Freiberg University of Mining and Technology, Freiberg D-09596, Germany
[b]Department of Stochastics, Freiberg University of Mining and Technology, Freiberg D-09596, Germany

Received 18 December 2001; accepted 4 November 2002

Abstract

The influence of the spatial arrangement of aggregates on the cold crushing strength (CCS) of refractory castables is studied by means of methods of point process statistics. Two series of self-flowing refractory castables differing in the kind of aggregates used (tabular alumina, corundum balls) are analysed using quantitative image analysis and methods of spatial statistics. Their spatial variability is described by means of the pair correlation function (pcf) and the density function of the nearest neighbour distance (nnd) distribution. It is shown that both characteristics, pcf and nnd, are in close correlation with CCS.

Keywords: Aggregate; Mechanical properties; Image analysis; Statistics

1. Introduction

It is well known in materials science that for many materials, there are close relationships between bulk material properties and geometrical microstructure. This is of large practical value since the geometrical structure can be easily studied, interpreted, and related to production processes. One of the simplest known relationships is the direct proportionality for some metals between the Brinell hardness and the specific surface area of grain boundaries S_V [1]. A similar rule holds for ductile single-phase materials, in which the mean grain size plays a significant role in mechanical behaviour (e.g., finer grains promote a higher toughness) [2]. This rule could be regarded as a particular case of a general relationship between the specific surface area of grain boundaries S_V and the mechanical properties of metallic materials [3]. Many material scientists have studied such relationships for different materials and have developed related theories. It is known that spatial variability of geometrical structure plays an important role. ''In practical applications, the nonuniformity of the packing is likely to be of greater significance than any average property (Brown and Hawksley)'' (Stroeven [4], p. 113). The characterization of ''nonuniformity'' is a difficult task, which is often solved only qualitatively. It has been found that in some cases, homogeneous or regular structures were mechanically stronger than inhomogeneous or irregular ones. The present paper reconsiders this hypothesis for refractory castables using a quantitative approach by means of planar sections.

Self-flowing castables are composite materials consisting of two phases [i.e., a system of grains (refractory aggregates) embedded in a matrix (binding system) as the second phase]. A logic approach should be to describe the particle dispersion geometry by quantitatively applying the theory of point processes [3,5,6] to the system of grain centre points in planar sections. This approach can be refined by attributing ''marks'' to the points, characterizing size, shape, or orientations of the grains. In this paper, the nearest neighbour distance (nnd) distribution and the pair correlation function (pcf) are the main statistical tools. These functions offer an elegant description of the degree of inhomogeneity in point systems.

The pcf and the nnd distribution have been already used in materials science. The mean nnd was used for the study of the degree and character of inhomogeneity of grain structure in concrete (see Stroeven [7] and Stroeven and Stroeven [8–10]). These authors also used the pcf approach: In Ref. [11], they applied an integrated version of the pcf, the radial distribution function, to the analysis of fibre dispersions in steel fibre-reinforced concrete. The pcf

* Corresponding author. Tel.: +49-3731-39-2118; fax: +49-3731-39-3598.
E-mail address: stoyan@orion.hrz.tu-freiberg.de (D. Stoyan).

0008-8846/02/$ – see front matter © 2002 Elsevier Science Ltd. All rights reserved.
doi:10.1016/S0008-8846(02)01056-6

appeared also in the study of metallic structures [12]. Petrov and Schlegel [13] used the pcf for describing the structure of macropores of three different kinds of autoclaved aerated concrete. They related the form of the pcf to the density of samples and noticed that a higher density of autoclaved aerated concrete leads to a higher and sharper primary maximum and to sharper peaks of the pcf. But these two papers used only qualitative differences of pcfs to compare different structures. Quantitative statements based on pcfs were obtained by Stoyan and Schnabel [14]. They discussed the relationship between the pcf and the arrangement of grains of alumina ceramics and introduced a parameter for describing the shape of the pcf. It was shown that this parameter is closely related to the mean bending strength of alumina ceramics. One step further was taken by Kalmykov et al. [15], who investigated the spatial arrangement of particles for revealing the type of interaction between particles in the course of phase separation. They determined the pcf of centres of precipitated particles in sodium borosilicate glass using experimental data from planar sections. The approach of the present paper is similar to that of Stoyan and Schnabel [14].

2. Materials

Self-flowing refractory castables have a consistency after mixing, allowing them to flow and become compact without the application of external energy. The binding system is decisive for refractoriness of the castables, whereas mechanical strength depends mainly on the aggregates.

Two series of refractory castables, differing only in the kind of aggregates, were studied:

Series A—aggregates of tabular alumina (fraction 1.0–3.0 mm from Alcoa); and
Series B—aggregates of corundum balls (fraction 1.5–2.5 mm from Mühlmeier).

For both series, samples with three different volume fractions of aggregates (50, 55, and 60 vol.%) were prepared. The binder consisted of high alumina cement (Secar 71; Lafarge), ultrafine alumina (CT3000SG; Alcoa), and superplasticizer (Darvan 7S; Vanderbilt), and was identical for both Series A and B. Similar preparation and testing conditions were maintained for all samples.

3. Experimental

3.1. Preparation of castable samples

All ingredients were dry-mixed for 4 min in a Hobart mixer. After adding 20 vol.% of water (the same amount of water was used for all specimens), another 4 min of wet mixing followed. The consistency of fresh castables was expressed by the flow measure according to ASTM C 230. The fresh castables were cast into moulds without compaction or vibration, and cured for 24 h in a curing chamber (room temperature and 90% RH). After demoulding, the samples were dried at 110 °C for 24 h. Finally, the samples were fired at 1000 °C for 5 h. The heating rate was 4 K/min.

3.2. Measurement of cold crushing strength (CCS)

The measurement of CCS was carried out with five cylindrical samples 50 mm in diameter and 50 mm in height. The specimens were subjected to direct compression between two steel platens in a load-controlled testing machine in accordance with preliminary standard ENV 1402. The sample deformation of 0.5% was employed to define the rupture load. The loading rate was 1 MPa/s.

The CCS of refractory castables is defined as the rupture load that the castables withstand at room temperature per unit of area of the top and bottom surfaces of the specimen. CCS is a complex characteristic reflecting preparation and testing method, specimen geometry, and material properties. Hence, it is influenced by many factors, as indicated by Stroeven [4]. Mechanical properties are governed by imperfections in aggregate structure, in the structure of matrix, and along the interface zone. The size of aggregates also plays a role because it is crack interaction that governs the process of crack coalescence, which finally leads to rupture.

3.3. Preparation of samples for image analysis

Various sections of the cylindrical samples were prepared for macrostructural examination by standard ceramographic procedures [16]. The structure of samples was revealed by applying black paint to the section, followed by a polishing operation. This yields a black (matrix) and white (aggregate section profiles) image. Next, digital images were obtained using a video camera and a framegrabber card. These images were binarized by setting appropriate threshold levels. Small disturbing objects were removed by subjecting the binary images to opening operation (i.e., a combination of erosion and dilation transformation) [3]. These images were finally quantitatively analysed using automatic image analysis.

3.4. Determination of profile centres

For the section profiles, the centres were determined automatically using the Image C-MATAN software of IMTRONIC (see Figs. 1 and 2). The ‘‘centres’’ are defined as centres of the circumscribed quadrangles oriented parallel to the frame of the field, and not as centres of gravity. This definition of centres was dictated by the software. In the case of circular profiles, there is no difference, whereas

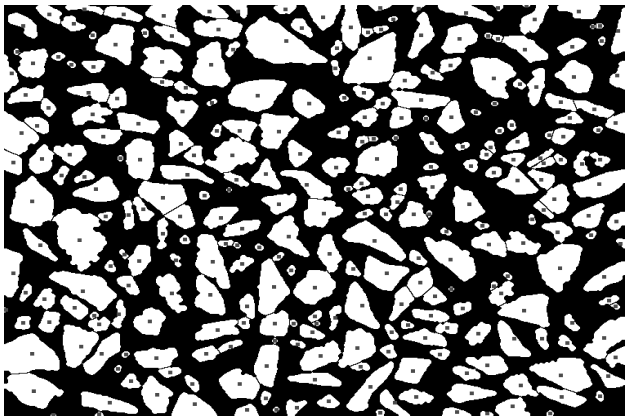

Fig. 1. Binary image of A55 (55 vol.% of tabular alumina—Series A) with marked centres of aggregates.

otherwise, the centre-of-gravity definition will lead to somewhat shorter distances.

4. Methods

4.1. The nnd distribution

In this paper, use is made of the centres of grain section profiles in planar sections, which are considered as a sample of a point process. An important characteristic of point processes, which can be employed for describing empirical point patterns, is the nnd distribution function $D(r)$. Let x be a randomly selected point of a planar point process. Then $D(r)$ is the probability that the smallest distance from x to any of its neighbouring points is smaller than the argument r. $1-D(r)$ is the probability that in the circle $b(x,r)$ with radius r and centred at the point x, there is no further point of this point process. The corresponding density function is denoted by $d(r)$. A similar reasoning can be given for the spatial case.

Various methods exist for the statistical estimation of $D(r)$ and $d(r)$ [3,5,17]. A naive method of a statistical estimation of $D(r)$ is to determine for each point of the pattern the nearest neighbour, whereupon the corresponding distance is measured. All these distances form a sample, which can be analysed by the classical methods of statistics (see Stoyan and Stoyan [6], p. 296; Ohser and Mücklich [3], p. 288). Of course, the determination of $d(r)$ is made in practice by means of computers. We used the STG software developed at the Department of Stochastics at the Freiberg University of Mining and Technology for the estimation of the nnd density function.

4.2. The pcf

The pcf plays also an important role in statistics for planar as well as spatial point processes. In the planar case, it can be explained as follows. Let λ denote the planar point density, the mean number of profile centres per unit area. The probability to find a point in an infinitesimally small circle of area dA is λdA. Consider now two small circles with respective areas dA_1 and dA_2 and a centre-to-centre distance r. If $P(r)$ is the probability that the two circles contain both a point of the point process, then $P(r)=\lambda^2 g(r)dA_1dA_2$, in which $g(r)$ is the so-called pair correlation function.

For a completely random point process (i.e., a so-called homogeneous Poisson process), $g(r)=1$ for all r, since in this case, the events to have points in the two circles are independent. However, such a point process will not be a good model for a grain system in refractory castables. Instead, the pcfs for such structures will have a complex form.

The pcf characterizes the frequency of distances between points. A typical pcf reveals maxima and minima as indicated by Fig. 3. The maxima of $g(r)$ characterize preferred distances, whereas the minima of $g(r)$ represent rarely occurring distances. Point pattern representations of particle system have a hard core distance r_0 (i.e., distances smaller than r_0 are impossible). Suitable parameters of $g(r)$ characterize the degree of order of the corresponding structure as shown by Stoyan and Stoyan [6] (p. 251).

The present paper uses a new order parameter O, defined by:

$$O=\frac{g(r_1)}{r_1-r_0},$$

where r_1 is the position, $g(r_1)$ is the value of the first maximum of the pcf, and r_0 is the hard core distance. The parameter O characterizes the average growth rate of the pcf between r_0 and r_1. A larger value of the parameter O indicates a lower degree of inhomogeneity in the structure.

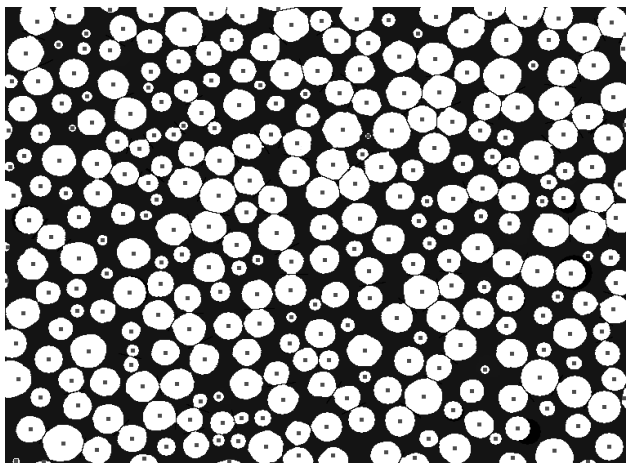

Fig. 2. Binary image of B55 (55 vol.% of corundum balls—Series B) with marked centres of aggregates.

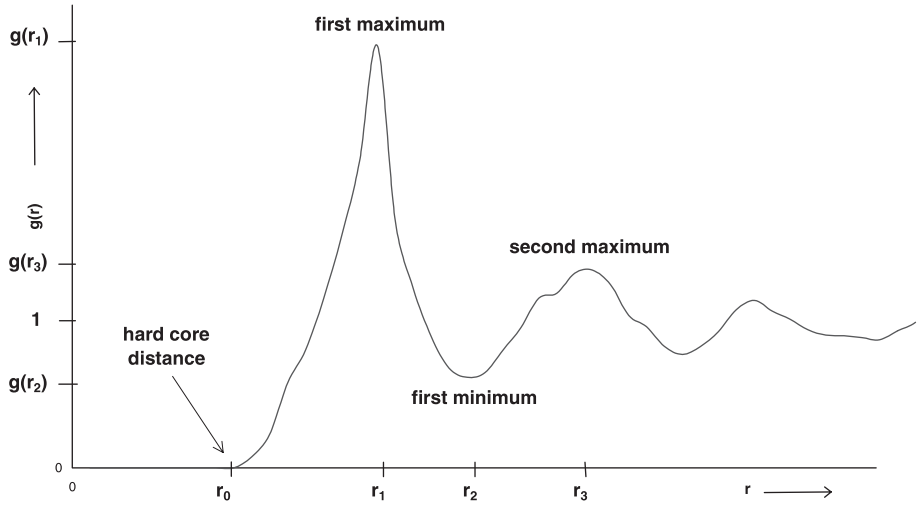

Fig. 3. Idealized pcf with marked significant extremes.

The statistical determination of the pcf is described in the literature [3,5,18]. All point pairs of the pattern are considered and relevant distances are determined by a so-called kernel function k. In the present case, use is made of the Epanechnikov kernel:

$$k(r) = \frac{3}{4h}\left(1 - \frac{r^2}{h^2}\right), \qquad (-h \le r \le h),$$

and $k(r) = 0$ otherwise [5]. Herein, h is a bandwidth parameter, defining the width of the kernel function. Its choice is crucial for the quality of the estimated pcf. When h is too small, the experimental pcf will reveal an excessive amount of structural details, as reflected by Fig. 4. Contrary, the experimental pcf will be smooth for large h, but in this case, important structural information about the point pattern is lost, as demonstrated by Fig. 5. The optimum bandwidth parameter h should be assessed in a preliminary investigation. A recommendation for the choice of h is given in Ref. [6], p. 285. For all statistical analyses of this paper, the value $h = 0.4$ mm was used for $r < 3.5$ mm and $h = 1$ mm for larger r.

For distances r smaller than the hard core distance r_0, the pcf has to be equal to zero. But statistical estimates obtained with kernel function can lead to non-zero values for $r < r_0$. Therefore, to ensure that $g(r) = 0$ for $r < r_0$, the reflection method was employed (Ref. [6], p. 368). Also for the estimation of the pcf, the STG software was used.

5. Results

5.1. CCS

The dependence of CCS on volume fraction of tabular alumina (Series A) is shown in Fig. 6. The relationship between CCS and volume fraction is far from linear, and

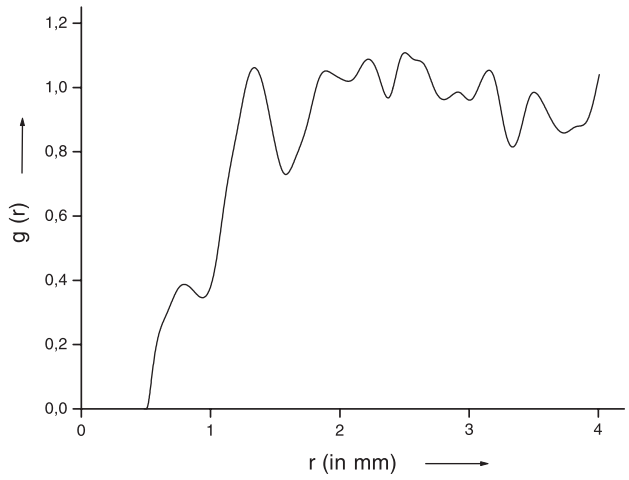

Fig. 4. The pcf estimated with a too small bandwidth parameter h.

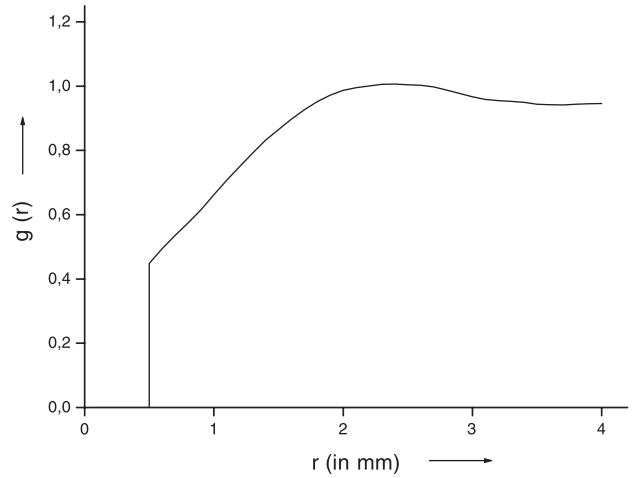

Fig. 5. The pcf estimated with a too large bandwidth parameter h (for the same point field as in Fig. 4).

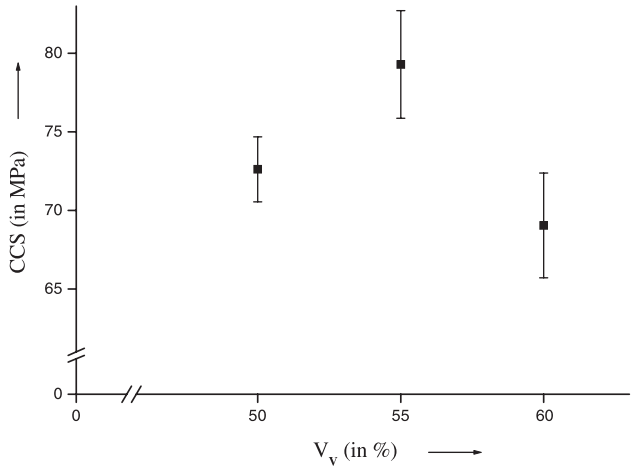

Fig. 6. Dependence of CCS on aggregate volume fraction of Series A.

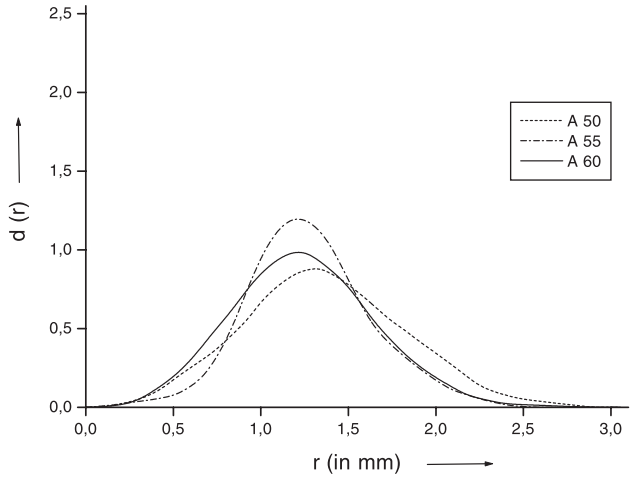

Fig. 8. Density function of the nnd for the samples of Series A.

instead reveals a maximum at 55 vol.% of aggregates A. In contrast, the results for the Series B displayed in Fig. 7 show an almost linear dependence.

During the testing of CCS, the formation of a few small cracks in the direction of the applied load was observed. The propagation of these cracks, followed by the formation of some secondary cracks perpendicular to the applied load, finally led to gradual rupture of the samples. The failure of the specimens took place approximately in the middle of the height because of the minimum effect of the frictional forces here. No differences were observed in the formation and propagation of cracks between samples with different volume fraction of aggregates.

5.2. Point process statistics

Fig. 8 shows the estimated density functions of the nnd for the samples of Series A. As expected, the means m_D of the density functions shift with higher volume fraction of aggregates to lower values of r, but the differences are small, as shown in Table 1. In contrast, the variances of the curves show remarkable differences, as revealed by the corresponding standard deviations (S.D.) in Table 1. The highest value of S.D. was found for Curve A50, whereas the smallest appeared for Curve A55. Thus, it can be concluded that the samples for Curve A55 have the lowest degree of structural inhomogeneity.

Fig. 9 shows the estimated density function of the nnd for the samples of Series B. A higher volume fraction of aggregates is reflected by a negligible shift of m_D to lower values of r. In contrast to Series A, the value of S.D. decreases with increasing volume fraction of aggregates.

Fig. 10 shows experimental pcfs for three volume fractions of tabular alumina (A50, A55, and A60) of Series A. The three curves are averages of three independent trials. The form of the curves for small values of r is clearly different from that of the Poisson process. The corresponding parameters are given in Table 1. The minimum distance r_0 and the values of $g(r_1)$ are similar for all three pcfs, but there are differences in the preferred distance r_1.

The form of the curve for A55 differs significantly from the others. The maximum of $g(r)$ for A55 is found at a smaller interpoint distance (i.e., the value is about 1.40 mm, whereas 2.39 and 3.35 mm appear for A50 and A60, respectively). Qualitatively, curves A50, A55, and A60 are

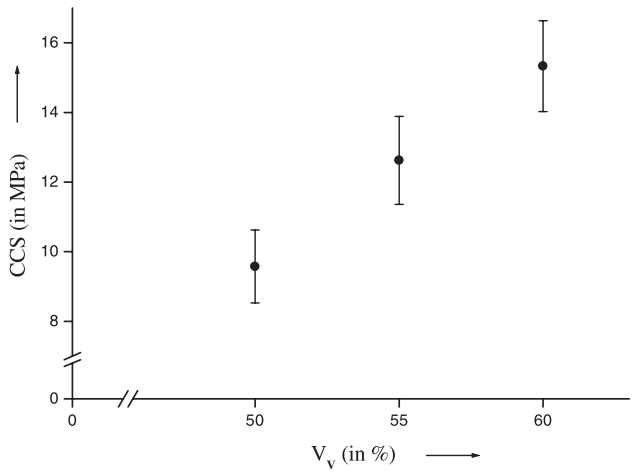

Fig. 7. Dependence of CCS on aggregate volume fraction of Series B.

Table 1
Characteristics of the pcfs and the nnd functions for Series A

	r_0	r_1	$g(r_1)$	O	m_D	S.D.	V
A50	0.39	2.39	1.111	0.56	1.34	0.43	0.32
A55	0.40	1.40	1.107	1.11	1.28	0.31	0.24
A60	0.35	3.35	1.092	0.61	1.25	0.38	0.30

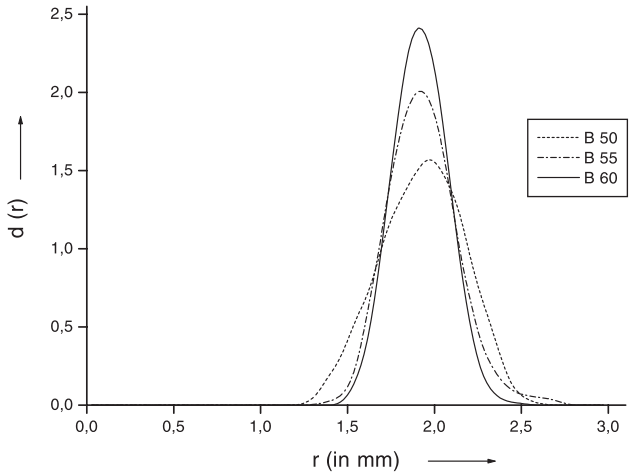

Fig. 9. Density function of the nnd for the samples of Series B.

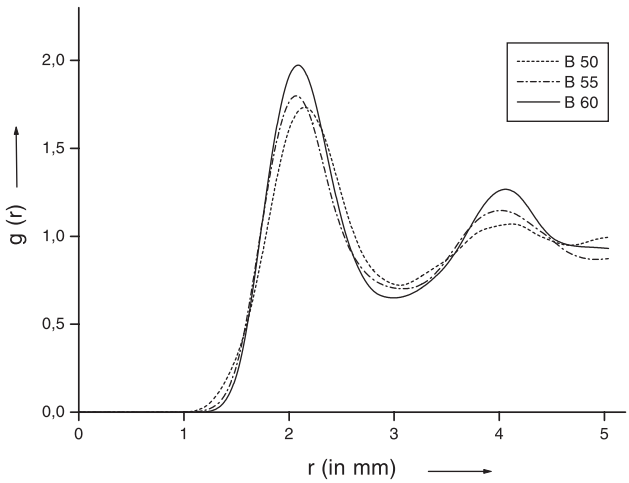

Fig. 11. Experimental planar pcf $g(r)$ for the samples of Series B.

between the pcf of a Poisson process and of a process with weak short-range order, the so-called soft core point process (Ref. [6], p. 258). The curve of A55 shows the highest short-range order. This is expressed quantitatively by the higher value of the order parameter O (i.e., 1.11 for A55 as compared to 0.56 for A50 and 0.61 for A60).

Fig. 11 presents the pcfs of Series B. The corresponding curves for B50, B55, and B 60 reflect all a low degree of inhomogeneity. There are two clear maxima for each curve corresponding to the distances to the first and second neighbours. At increasing r, all curves approach the value 1. The form of the pcfs for B50, B55, and B60 is similar; only the preferred distances differ. With increasing volume fraction of corundum balls, the maximum of pcfs increases, while the maximum moves to smaller values of distances. Consequently, the order parameter O increases with increasing volume fraction in the measured range.

The curves in Figs. 10 and 11 reflect clear differences in the geometrical structure of the point patterns of grain centres. Whereas for Series B there is a low degree of inhomogeneity and even a tendency to order, for Series A the pattern is rather variable and inhomogeneous; the flat shape of many grains enables very short interpoint distances.

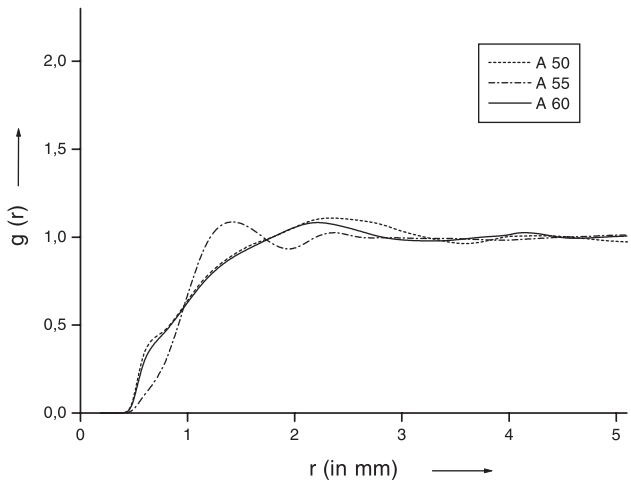

Fig. 10. Experimental planar pcf $g(r)$ for the samples of Series A.

6. Evaluation

A comparison of the values of the CCS of refractory castables presented in Figs. 6 and 7 with the values of the order parameter O of the pcfs shows that there is a close relationship between O and CCS. High values of CCS appear when the values of O are high. Similarly, the variance of the density function of nnd correlates with CCS: High values of CCS appear when the variance values are small. Both characteristics, pcf and nnd, reflect the short-range order in the structure and correlate with CCS. However, the present paper is not a micromechanical paper. It describes an interesting phenomenon by means of geometrical–statistical methods, but does not intend to give a theoretical explanation in terms of micromechanics.

Increasing grain density leads to an interaction of the grains. As Fig. 1 shows, there are some pairs of opposite sides of grains that are nearly parallel. This is a form of *local* anisotropy that cannot be measured by means of roses of intersections. The roses of intersections determined for the samples did not show a significant amount of *global* anisotropy. Implicitly, local parallelism is also expressed by the pcf; the very short intergrain distances reflected by the pcf of A60 should involve parallel grain sides.

A potential alternative concept could be the use of specific surface area S_V. However, this is not helpful in

the context of the present paper, and therefore S_V was not determined. All aggregates of the same series are taken from the same bulk content. Hence, mean volume $\overline{V}$ and mean surface area $\overline{S}$ are identical, apart from natural scatter. Thus,

$$V_V = \overline{V} N_V$$

and

$$S_V = \overline{S} N_V,$$

where N_V is the mean number of grains per volume unit. That means that the ratio of S_V and V_V is a constant for a given particle geometry. Consequently, S_V cannot do a better job than V_V in explaining the differences in CCS for Series A. (Of course, it can explain the differences between Series A and B; the irregular shape—and thus their large specific surface area—of the grains in Series A will have caused the relatively high CCS values in this series.)

The investigations presented in this paper are based on planar sections of specimen. This does, of course, not yield complete spatial information, which could be obtained, for example, by computer tomography. Nevertheless, spatial characteristics derived from planar sections are closely related to spatial characteristics of the corresponding three-dimensional structure. For example, in the case of spherical grains and isotropy, stereology offers precise mathematical relationships between the pcf of the centres of the circular section profiles and the pcf of the sphere centres [5,19,20]. (To be precise, this technique belongs to second-order stereology. Classical first-order stereology offers methods for the determination of S_V or sphere diameter distribution functions from planar or linear sections.)

7. Conclusions

This paper shows that the spatial arrangement of the aggregates in castables reflected by point process characteristics has a significant influence on CCS. In this context, the shape of particles also plays an important role. Spherical particles can take arbitrary relative positions because of their ideal shape; with increasing volume fraction, the degree of inhomogeneity in systems of spheres decreases. This corresponds to increasing values of CCS. If the particles are not spherical, the situation is more complicated. There the structure with minimum degree of inhomogeneity and maximum CCS values can appear at medium values of volume fraction. The developed geometrical parameter O seems to be useful for characterizing the degree of inhomogeneity.

Acknowledgements

The authors thank Prof. P. Stroeven and an anonymous referee for a series of very constructive remarks on earlier versions of this paper. Prof. Hessenkemper was so kind to direct attention to S_V. The first author would also like to thank Mrs. Gudrun Heinzel for technical help.

References

[1] F.N. Rhines, Microstructology, Dr. Riederer-Verlag, Stuttgart, 1986.
[2] T.H. Courtney, Mechanical Behavior of Materials, McGraw-Hill, Boston, 2000.
[3] J. Ohser, F. Mücklich, Statistical Analysis of Microstructures in Materials Science, Wiley, Chichester, 2000.
[4] P. Stroeven, Some Aspects of the Micromechanics of Concrete, PhD Thesis, Delft University of Technology, Delft, 1973.
[5] D. Stoyan, W.S. Kendall, J. Mecke, Stochastic Geometry and Its Applications, Wiley, Chichester, 1995.
[6] D. Stoyan, H. Stoyan, Fractals, Random Shapes and Point Fields. Methods of Geometrical Statistics, Wiley, Chichester, 1994.
[7] P. Stroeven, Stereometric analysis of structural inhomogeneity and anisotropy of concrete, in: H.E. Exner (Ed.), Quantitative Analysis of Microstructures in Medicine, Biology and Material Development, vol. 5, Dr. Riederer-Verlag, Stuttgart, 1975, pp. 291-307. Special Issues of Practical Metalography.
[8] M. Stroeven, P. Stroeven, Computer-simulated internal structure of materials, Acta Stereol. 15 (3) (1996) 247–252.
[9] P. Stroeven, M. Stroeven, Size of representative volume element of concrete assessed by quantitative image analysis and computer simulation, Image Anal. Stereol. 20 (Suppl. 1) (2001) 216–220.
[10] P. Stroeven, M. Stroeven, Reconstructions by SPACE of the interfacial transition zone, Cem. Concr. Compos. 23 (2001) 189–200.
[11] P. Stroeven, M. Stroeven, Stereological characterization of fibre dispersions in concrete, Acta Stereol. 14 (1) (1995) 5–16.
[12] D. Stoyan, K. Wiencek, Spatial correlations in metal structures and their analysis, Mater. Charact. 26 (1991) 167–176.
[13] I. Petrov, E. Schlegel, Application of automatic image analysis for the investigation of autoclaved aerated concrete structure, Cem. Concr. Res. 24 (5) (1994) 830–840.
[14] D. Stoyan, H.-D. Schnabel, Description of relations between spatial variability of microstructure and mechanical strength of alumina ceramics, Ceram. Int. 16 (1990) 11–18.
[15] A.E. Kalmykov, M.P. Shepilov, G.A. Sycheva, Electron microscopic investigation of spatial ordering of particles formed in the course of liquid phase separation in sodium borosilicate glass, Glass Phys. Chem. 26 (3) (2000) 307–309.
[16] G. Petzow, Metallographic Etching, ASM International, Metals Park, OH, 1999.
[17] D. Stoyan, H. Stoyan, A. Tscheschel, T. Mattfeldt, On the estimation of distance distribution functions for the point processes and random sets, Image Anal. Stereol. 20 (Suppl. 1) (2001) 65–69.
[18] D. Stoyan, H. Stoyan, Improving ratio estimators of second order point process characteristics, Scand. J. Statist. 27 (2000) 641–656.
[19] K.-H. Hanisch, Stereological estimation of second-order characteristics and of the hard-core distance of systems of sphere centres, Biom. J. 25 (1983) 731–743.
[20] K.-H. Hanisch, D. Stoyan, Stereological estimation of the radial distribution function of centres of spheres, J. Microsc. 122 (1980) 131–141.